PIV and LDA measurements of the wake behind a wind turbine model

I V Naumov[1], R F Mikkelsen[2],V L Okulov [1,2] and J N Sørensen[2]

[1] Institute of Thermophysics, SB RAS, Novosibirsk 630090, Russia
[2]Department of Wind Energy, Technical University of Denmark, 2800 Lyngby, Denmark

E-mail: naumov@itp..nsc.ru

Abstract. In the present work we review the results of a series of measurements of the flow behind a model scale of a horizontal axis wind turbine rotor carried out at the water flume at Technical University of Denmark (DTU). The rotor is three-bladed and designed using Glauert theory for tip speed ratio λ =5 with a constant design lift coefficient along the span, $C_{Ldesign}$= 0.8. The measurements include dye visualization, Particle Image Velocimetry and Laser Doppler Anemometry. The wake instability has been studied in the range λ =3 - 9 at different cross-sections from the very near wake up to 10 rotor diameters downstream from the rotor. The initial flume flow was subject to a very low turbulence level with a uniform velocity profile, limiting the influence of external disturbances on the development of the inherent vortex instability. Using PIV measurements and visualizations, special attention was paid to detect and categorize different types of wake instabilities and the development of the flow in the near and the far wake. In parallel to PIV, LDA measurements provided data for various rotor regimes, revealing the existence of three main regular frequencies governing the development of different processes and instabilities in the rotor wake. In the far wake a constant frequency corresponding to the Strouhal number was found for the long-scale instabilities. This Strouhal number is in good agreement with the well-known constant that usually characterizes the oscillation in wakes behind bluff bodies. From associated visualizations and reconstructions of the flow field, it was found that the dynamics of the far wake is associated with the precession (rotation) of a helical vortex core. The data indicate that Strouhal number of this precession is independent of the rotor angular speed.

1. Introduction

Rotor systems such as wind turbines, hydro-turbine rotors, airplane and marine ship propellers generate complex wakes containing helical vortex structures. Wind turbine blade rotation produces a wake, which is the result of complex dynamics and interactions between different vorticity structures. The evolution and breakdown dynamics of these helical vortices is not fully understood and is also of fundamental interest in vortex dynamics. The connection between the vorticity structure formation in the near wake and the turbulence decay in the far wake is still an open question [1]. Fundamental studies on helical vortices have shown that their symmetrical helical structure is unstable to small perturbations. For wind turbines, these helical vortices play an important role in the development of the wake directly downstream of the rotor (the near-wake) and their evolution and breakdown dynamics influence the characteristics of the resultant far-wake many rotor diameter downstream [1]. In the case of three-bladed horizontal-axis wind turbines (HAWTs), vortices form in the tip and root

Content from this work may be used under the terms of the Creative Commons Attribution 3.0 licence. Any further distribution of this work must maintain attribution to the author(s) and the title of the work, journal citation and DOI.
Published under licence by IOP Publishing Ltd

region in the wake of each blade, resulting in three counter-rotating pairs of helical vortices. Experimental PIV measurements and flow visualizations [2-4] and numerical simulations [5] have all shown that the tip vortices of a wind turbine undergo pairing, with a resulting entanglement and merging of vortices.

A complete study of the corresponding flow structures downstream a marine ship propeller and wind rotor wakes was based on velocity visualizations in combination with LDA, hot-wire anemometers or acoustic Doppler velocimeter measurements for velocity field with phase averaging. It was found that downstream with respect to the destabilization of the helicoidal tip vortices the hub vortex also becomes unstable. By proceeding further downstream, the hub vortex starts oscillating sinusoidal, according to a spiral geometry, until breakdown occurs [6]. A low-frequency instability is also detected from wind tunnel tests of wind turbine models [7, 8]. In [9] this low-frequency instability, called wake meandering or wandering, is equal to 0.29 times the hub rotational frequency, and is ascribed to transversal oscillations of the wind turbine wake, which may be excited by the vortex shedding from the rotor disc in a similar way as for bluff bodies. The authors tried to deduce an empirical dependency of the Strouhal number as a function of trust, tip speed ratio, and number of blades. This low frequency is found to decrease with increasing tip speed ratio of the turbine and with increasing thrust coefficient. In works [8, 10], the low-frequency spectral component connected to wake meandering is equal to 0.34 times of the hub rotational frequency, and it can be detected up to a downstream distance of 1.5*d*, where *d* is rotor diameter.

Dimensionless numbers are important in fluid mechanics because their constancy can imply dynamic similarity between different flow regimes. A dimensionless parameter that describes the wake kinematics in flows around bodies is the Strouhal number

$$St = f\,D/U \tag{1}$$

where ***f*** is the frequency of the main oscillation in the wake; *D* is the body size and *U* is the free stream velocity. A unique value of the Strouhal number at about 0.2 is known to govern vortex shedding behind a sphere, where a helicoidal vortex structure appears in the wake [12] within a wide range of Reynolds numbers ($800 < Re < 200000$). Here the Reynolds number is defined as $Re=\rho UD/\mu$, where ρ is the fluid density and μ is dynamic viscosity. Another interesting feature of the Strouhal number is that it increases for bluff bodies when their size in the flow direction becomes larger than the cross-sectional dimension [11].

Recent investigations of rotor wake instabilities have shown the existence of a Strouhal number about 0.28 [7]. In this study, carried out for a tip speed ratio (λ) of 5.8, the dominant periodic oscillations were shown to appear in the spectra for the axial flow component in a single point about four rotor diameters downstream in the wake. Measurements on a scaled three-bladed horizontal axis wind turbine model was performed in work [13] where the wake flow near the rotor was investigated using Stereoscopic PIV. To analyze the dynamics of the wake, Proper Orthogonal Decomposition (POD) was applied on each series of snapshots. The POD analysis and determination of spectrum peaks for the first modes reconstruction coefficient was made for the combination of positions along rotor axis and tip speed ratios. For positions more than 3*d* the Strouhal number of the precessing wake was found independent of the rotor angular velocity and is in almost all cases close $fd/U= 0.22$. However, the POD analysis is not done under optimal conditions. The measurements plane does not cover a full cross section of the wake. This means that the full dynamics of the wakes is not captured. The number of samples (≈ 400) are relatively small both for the convergence of the POD modes, especially because the POD modes are not uncorrelated.

The current paper investigates the wake of a three-bladed HAWT rotor, with a blade design based on the Glauert [14] optimum rotor. The purpose of the present investigation is to determine the wake instability and properties of the Strouhal number observed in the far wake behind a wind turbine rotor. Compared to the flow around a bluff body, it is, however, rather difficult to discriminate between the various dynamic properties of the far field behind a rotor. The low-frequency behaviour encountered

in the flow behind a wind turbine is often referred to as wake meandering [15]. The notation of wake meandering usually refers to the low frequency movement of the wake due to large scale fluctuations of the incoming atmospheric turbulence. However, the large turbulent structures which belong to the atmospheric boundary layer, do not appear in wind or water tunnel experiments and the 'meandering' process in the wake behind model rotors is therefore most likely associated with vortex shedding. This is not fully understood, and the various types of instabilities may be of quite different nature.Therefore, in the present study, special attention has been paid to detect and categorize the various types of wake instabilities. This is accomplished by combining flow visualizations, LDA measurements and PIV-based reconstructions of the flow field. The objective of the current work is complex PIV and LDA investigation [16, 17] of the wake instability in the range $\lambda = 3 - 9$ at different cross-sections from the very near wake up to 10 rotor diameters downstream from the rotor.

2. Experimental Method

The three-bladed model rotor has a diameter d = 0.376m with blades of length 0.159m, consisting of SD7003 airfoil sections. The shape and pitch setting of the blade were calculated using the theory of Glauert [16] for optimum operating conditions at a tip speed ratio $\lambda = 5$, where $\lambda = \Omega R/U$, and Ω is angular speed of the rotor. The steady operating conditions e.g. wake profiles, measured power (C_P) and thrust (C_T) coefficient for $\lambda = 5$ was tested in detail [2, 3] with $C_P \approx 0.37$ and $C_T \approx 0.83$ at design $\lambda = 5$. The experiment took place in a water flume of length 35m, 3m width and an operative height of 0.9m. The 3m wide test section is fitted with transparent walls and the turbine model was installed at a distance of 20 m from the channel inlet. Three different flow regimes with free flow speeds U = 0.38m/s, 0.45m/s and 0.64m/s was investigated. The Reynolds numbers based on rotor diameter and free stream was varied in the range 140.000 <Re< 240.000. As working fluid, tap water at a temperature of 20ºC was used. In order to filter out disturbances the water was led through an inlet equipped with honeycomb. Prior to the experiment, the velocity profiles were measured at various positions in the flume in order to determine a cross section with as constant velocity as possible. Based on the measured velocity (figure 1 and figure 2) the rotor axis was positioned at a height of 0.5m from the channel bottom and 0.7m away from the flume walls. This diagram indicates that the velocity profile is constant 0.25m from the edges and across the flume in the region 0.25-0.65m above the bottom. The velocity profile variation of the incoming water flow is less than 1% during all experiments, measured with LDA and an independent OTT Z400 velocimeter. For PIV measurements the rotor axis was positioned at 1.5m away from the channel walls. The rotor was driven by a JVL Industri Elektronik MAC400 servo motor which was operated at a constant rotational speed within 2% accuracy. The torque of the motor was transferred to the rotor axis via a rigid gear transmission.

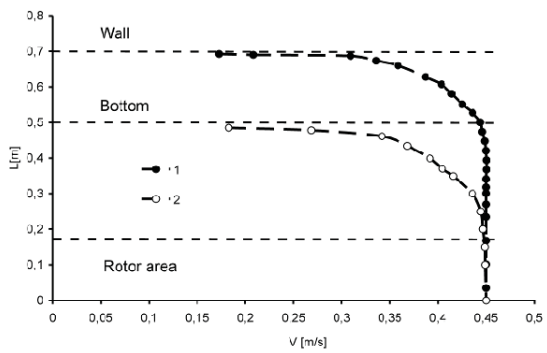

Figure 1. Free stream conditions (mean velocity) in the rotor cross section: average velocity profiles. 1 – from wall to rotor, 2 – from flume bottom to rotor.

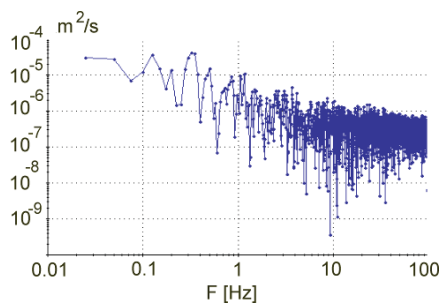

Figure 2. Spectrum of the free flow oscillations in the rotor area.

The angle of attack of the blade was fixed for each test case and corresponds to the geometry for a rotor. The flow downstream of the rotor develops into a well-defined 3D structure consisting of helical tip vortices which are visualized by fluorescence dye and by reconstruction from the velocity and vorticity field obtained by Stereoscopic Particle Image Velocimetry of the near wake (figure 3).

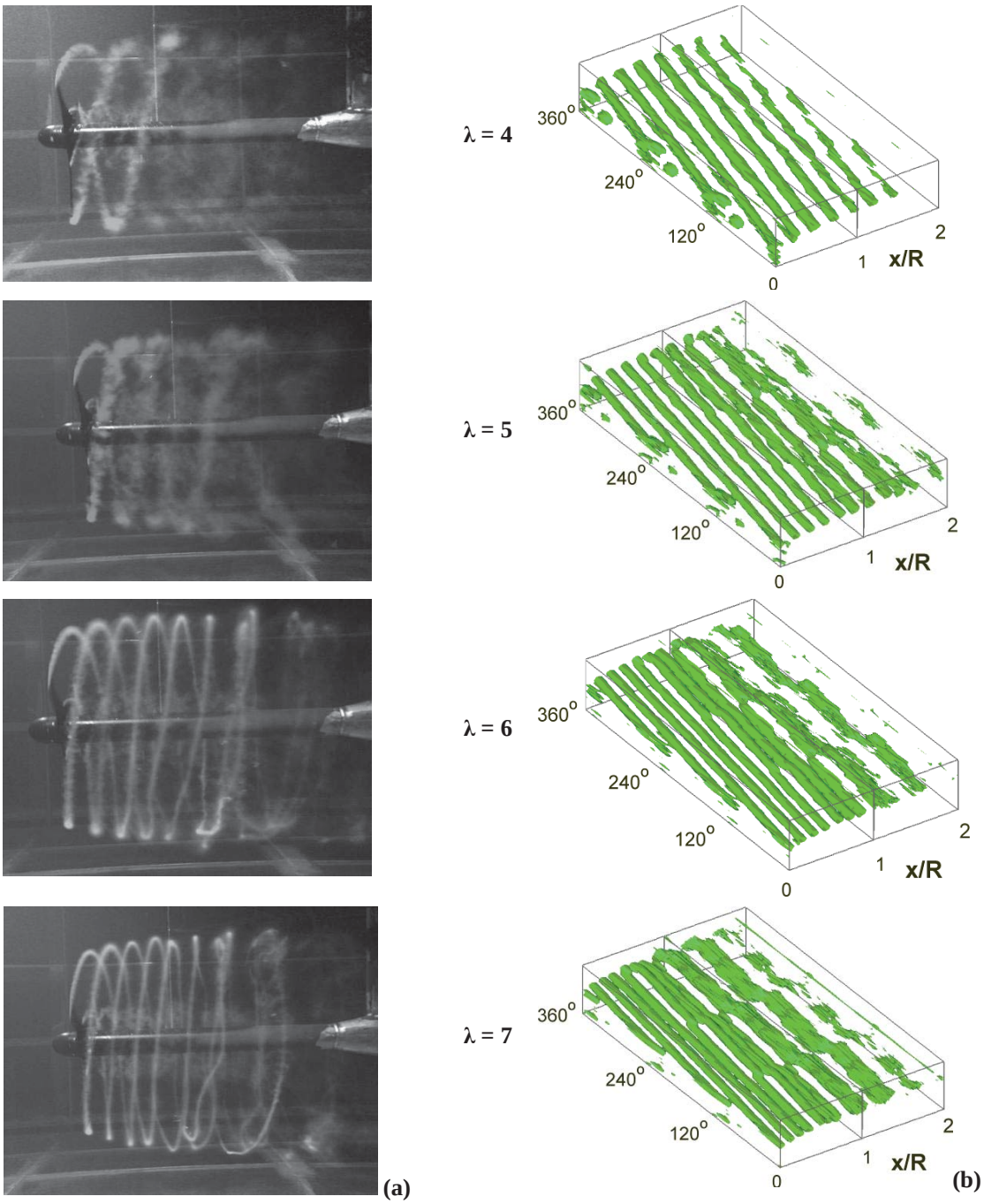

Figure 3. Visualization of the 3-D vortex structure behind rotor: a – dye visualization, b - representation of the tip vortex structure: 0-360 deg. with step 15 from PIV velocity fields.

The visualizations are however not useable to detect the flow structures in the far wake of the rotor because the initial helical structure disappears due to mixing when the vortices become unstable and starts pairing up [2, 3]. A more accurate recognition of the flow structures was obtained using LDA and Dantec Stereoscopic PIV (figure 4 and figure 5).

The regular movement of the vortex structures, as shown by the visualizations in figure 3, complicates extremely the ability of the PIV technique to analyze instantaneous flow patterns, because of unsteady variations in the resulting vector fields, which usually are reduced by averaging over a large amount of realizations. In swirling flows, averaging works well for stationary regimes and shows good agreement with other diagnostic tools and results from computer simulations. However, in the present case, when dealing with time-varying swirling wake flows, this type of averaging only provides mean features in which non-stationary behavior and instantaneous patterns are smoothened out. A solution to this problem is to perform phase-averaging of the dominating flow oscillations [17]. In accordance with this technique, LDA and PIV were combined. At first the dominant frequencies for each operating regime (λ; U) were obtained from LDA measurements. After then about 30 PIV samples in the same phase of the main oscillation were selected for an averaging from a random serial of 500 images. Thus, combining LDA and PIV using the above-described procedure, makes it possible to detect the main frequencies as well as their associated flow structures.

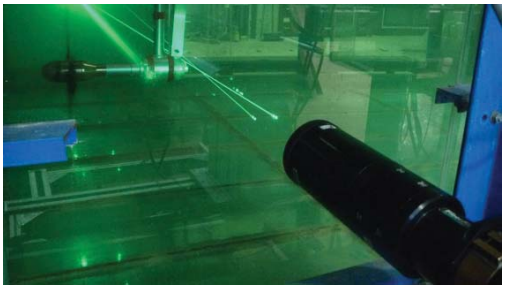

Figure 4. Photo LDA measurements of flow pulsation behind rotor.

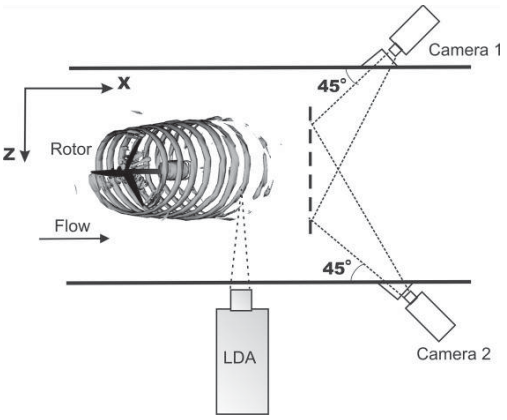

Figure 5. Sketch of LDA and SPIV measurements in cross section (at x=9R).

The PIV system determines the three velocity components in cross-section through a light sheet. The light source was a Nd:YAG laser producing 120mJ of energy in a single pulse at a wavelength of 532 nm and an operating frequency of 15Hz. A 2mm thick light sheet was directly towards the rotor in a horizontal plane. The images were recorded by two Dantec HiSense II cameras with 1344x1024 pixels resolution. The 3-D velocity field was calculated using Dantec Dynamic Studio 2.21 software. The cameras were placed perpendicularly to each other on the different sides of the flume and at angle of 45º to the walls (figure 5). Water-filled optical prisms were installed between the cameras and the test section to reduce the distortions from the camera inclination to the wall. Since the cameras were placed at an angle to the light sheet, the focus plane was adjusted using Scheimpflug adapters. In the cross-section directions the PIV area measured 0.22 x 0.35m, positioned about the center of the far wake.

To obtain more information about the wake development, the wake oscillations were measured with high temporal accuracy using LDA. These measurements were carried out through all wake area in the PIV-testing plane at different radial positions from the rotor axis (0.33R, 0.66R, 1R and 1.22R) with stream-wise steps of 0.2R (figure 6). In each point the local axial velocity history was obtained using a Dantec 2-D Fiber flow LDA, based on a 1W Argon laser with a differential optical

configuration with a frequency shift of 40 MHz. The diameter of the optical gauge is 112mm and the focal length is 600mm with a beam diameter of 1.35mm. The wavelength of the laser beam is 514.5 nm (green light). The size of the probing optical field was $0.12\times0.12\times1.52\text{mm}^3$. The signal from the light-scattering particles is collected and processed by a Burst Specter Analyzer (BSA57N2 commercial signal processor) to detect the characteristic frequencies in the flow. Each time history was recorded in a period of 60s, corresponding to about 20 - 50 rotor rotation. The recorded time histories were evaluated for their frequency content using spectral analysis.

3. Development of vortex system behind rotor

The dye tracers give a good impression of the structure of the tip vortices as seen in figure 3, which shows the tip vortices as continuous curves giving a nearly perfect helical shape with a slight expansion. The vortex pitch (distance between turns of the tip vortex) decreases at increasing tip speed ratios λ. These photos also indicate an onset of initial disturbances for all operating regimes in the early development of the wake (approximately $2R$ downstream) as well as the initial point of onset of the transitional regime to far wake. This happens approximately $4R$ downstream from the rotor, where a full mixing of the dye tracers is seen to take place. The mixing connects with the wake instability and may be explained as a transition from the onset of initial disturbances to a fully developed far wake. This is triggered by the mutual interaction between the individual tip vortices after which a strong non-linear interaction eventually generates small-scale turbulence and mixing. Due to the mixing in the far wake, the visualizations gave no information about the far wake behavior. As a consequence, to achieve a more accurate picture of the wake development, the visualizations were supplemented by LDA measurements in a number of points downstream of the rotor (see figure 6).

Initially the setup with non-rotating rotor, 90° pitch, was tested for the development of the oscillations in the wake region due to the support arm, that is, with the support arm extending in the normal direction to the plane where LDA measurements are obtained. At different points near the setup small changes was found in the spectra compared with the spectra of free stream flow (figure 2). The values of the main spectral components are approximately doubled by the influence of the support arm in the non-rotating rotor configuration. With the rotor operating ‘normally’, the spectral levels of the wake oscillations is significantly higher (figure 6). Thus, the disturbances from the mounting arms are quite small and can hardly be seen in the spectra on the same location (zone B). Analyzing the LDA-spectra of the axial velocity in the rotor wake confirmed the existence of different zones with different main frequencies. In the tested region the main flow oscillations have been determined to be associated with the blade and rotor frequencies as well as with a stable oscillation at a very low frequency in far wake area (figure 6). Examples of the spectra are presented in Figures 6 for regimes with $\lambda = 5$ and $U = 0.45$m/s. By analyzing the various spectra four different zones have been identified (figure 6): zone A, where the blade frequency dominates; zone B, where the rotor frequency dominates; zone C, which is dominated by both the rotor and blade frequencies plus various frequencies governed by the mutual interaction between the dynamics of the tip vortices and finally zone D, which is dominated by a low frequency that was observed at all downstream distances.

By characterizing the wake through the dominating frequencies, in opposition to the usual distinction between near wake and far wake, we here get four fundamentally different wake zones. Defining the near wake as the region in which the rotor aerodynamics can be felt, zones A, B and C all belong to this, whereas the spectra in zone D do not contain any traces of the rotor or blade frequencies. Instead zone D is dominated by a very low frequency mode, which was observed to be invariant for all operating regimes analyzed in the experiment (figure 7). The main flow oscillations frequencies have been determined and presented in table 1 for $U = 0.45$m/s and different λ. Table 1 shows examples of far wake frequency for the different tip speed ratios. It should be mentioned that for all tip speed ratios the LDA-spectra only contain this one significant frequency, demonstrating that the flow is governed by only one significant mode in the far wake. In all points of the far wake ($x > 5R$) this mode attains the same frequency, whereas a small variation in the frequency took place for different operating regimes in the transition range between the near and the far wake ($3R < x < 5R$).

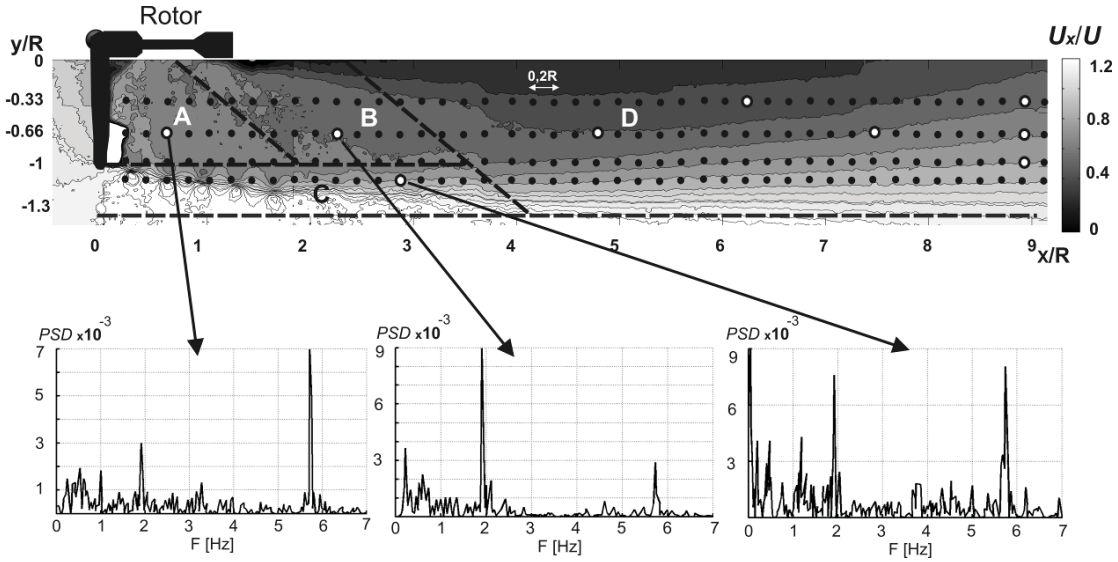

Figure 6. Points of LDA-tests and zones showing different frequencies of the main oscilations in the rotor wake with an examples of LDA-spectra: A, where the blade frequency dominates; B, where the rotor frequency dominates; C, which is dominated by both the rotor and blade frequencies and D is far wake without any traces of the rotor or blade frequencies.

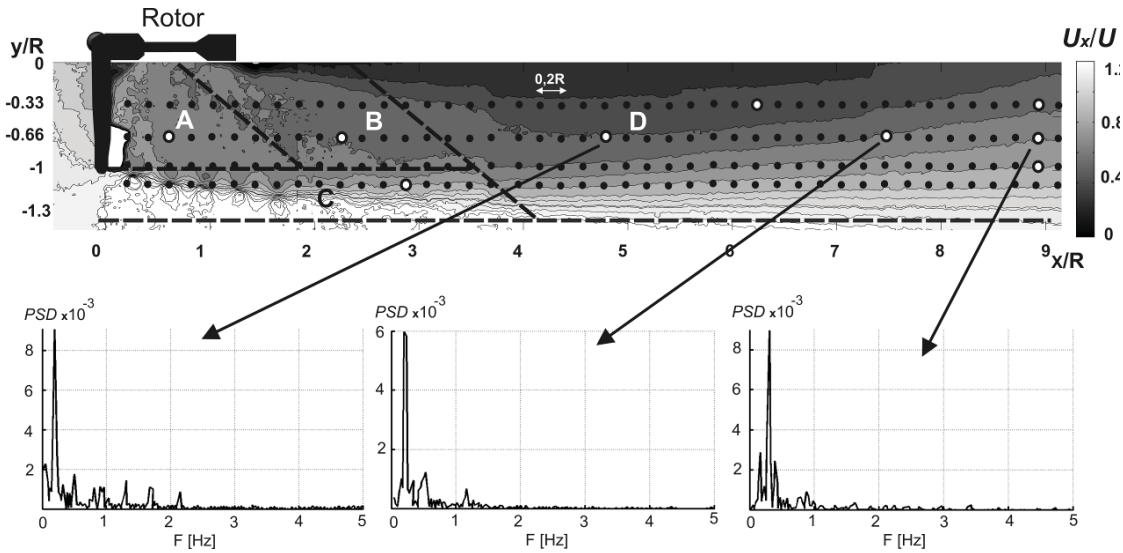

Figure 7. Examples of LDA-spectra in points of the far wake (zone D) on the same radial distance from the rotor axis of $r = 0.66R$ and at different points downstream: a) $x = 4.8R$; b) $x = 7.4R$ and c) $x = 9.0R$.

The work by Medici & Alfredsson [11] reported similar low frequency behavior in the near wake ($x = 2R$). This behavior is in accordance with our observations, although measured at different locations. Some distinction in the results is referred to the differences in design of the rotors, resulting in a different near wake vortex system. Flow oscillations dependency of the free stream speed outside along the wake was also tested.

Table 1. Spectral analysis for the tests performed by LDA with different TSR values at U = 0.45 m/s.

TSR	Near wake		Far wake at 9R
	F_{hub} (Hz)	F_{tip} (Hz)	F_{vortex} (Hz)
3	1,14	3,436	0,28
4	1,544	4,606	0,27
5	1,893	5,678	0,28
6	2,291	6,897	0,26
7	2,689	8,043	0,27
8	3,063	9,213	0,28
9	3,431	10,293	0,28

Here it was found that the dominant frequency changes linearly with the free stream velocity in zone D. However, using the definition eq. (1), it was found that the Strouhal number in the far wake is constant for all parameters (λ and U). Furthermore, the value of the Strouhal number is everywhere equal to St=0.23, which is in very good correlation with the usual Strouhal number of about 0.2 for bluff body vortex shedding (figure 8).

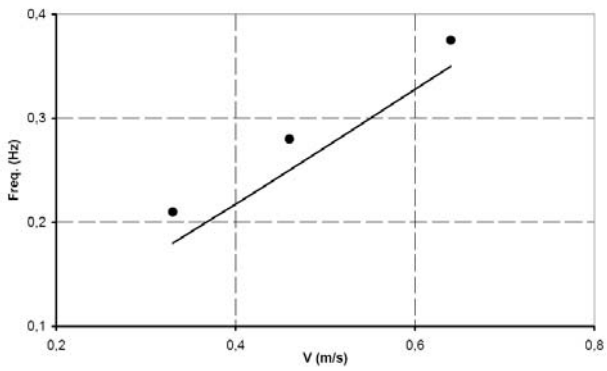

Figure 8. Examples of a frequency for (r = 0.66R; x=9R) in far wake (zone D) for different velocity of incoming flow. Solid line correspondet St = 0.2.

Besides the inherent dynamics of the helical vortex system, there are other external parameters that have an influence on instabilities and the dynamic behavior of large scale wind turbine wakes. The main external parameter is related to the wind conditions of the atmospheric boundary layer, where turbulence of many scales destroys the tip vortices and the interaction with the large coherent turbulent structures drives the large-scale fluctuations of the wake. This is usually referred to as wake meandering because the different wind conditions are assumed to disturb the axisymmetric wake. This has led to model development like the dynamic wake meandering model [16] which is based on the fundamental presumption stating that the transport of wakes in the atmospheric boundary layer can be modeled by considering the wakes to act as passive tracers driven by the large-scale turbulence structures. In our experiments the effect of external instabilities is excluded as the turbulence level in the flume is small, hence, only the self-induced part of wake instabilities can be analyzed. From the knowledge on flow about spheres the recirculation bubble of the near wake behind a sphere degenerates into large-scale vortex loops, which eventually develops into a helicoidal wake structures

in the far wake. It appears that the regular configuration of the tip vortices in the near wake (figure 3) plays a similar role as the recirculation bubble behind a bluff body. We may therefore, in the case of a wind turbine rotor, expect the generation of a precessing helical wake downstream of the near wake.

Figure 9 shows the instantaneous axial velocity field in axial cross sections for x =9R at different times. The amplitude of the wake center precession was 0.2R and the intensity of flow pulsation measured with LDA was less than 10% of incoming flow velocity. By reconstructing the flow field from the PIV measurements it is clearly seen that the far wake rotates in a way similar to a helicoidal vortex structure in the far wake behind a sphere. The meandering from large scale ambient turbulence varies depending on atmospheric stability. But in the case where the turbulence is so low (stable conditions offshore) this self induced wake precession could make a sizeable contribution to the unsteady loads affecting downstream positioned turbines in wind farms.

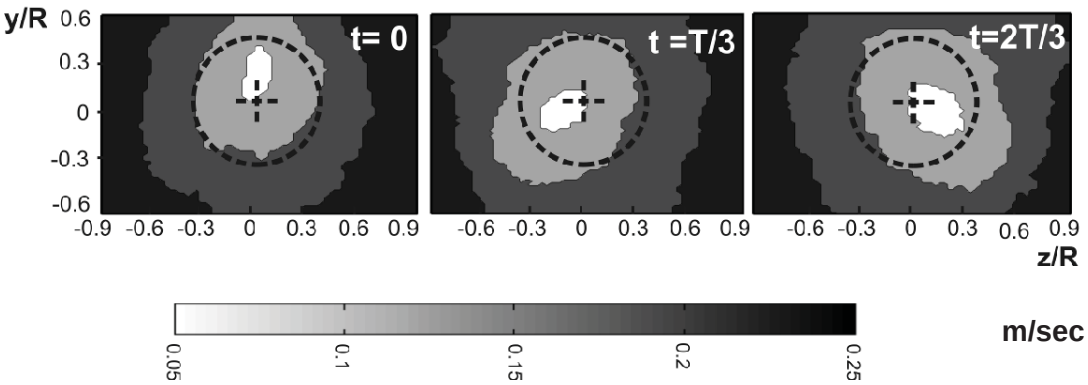

Figure 9. PIV-visualisation of a precession of the vortex structure in the rotor far wake at x=9R. The amplitude of the wake center precession was 0.2R.

4. Conclusions

The flow behind the model of a horizontal axis wind turbine rotor was investigated experimentally in a water flume. The measurements include visualization, PIV and LDA. The initial flume flow was subject to a very low turbulence level with a uniform velocity profile, limiting the influence of external disturbances on the development of the inherent vortex instability. The wake instability has been studied at different cross-sections from the very near wake up to 10 rotor diameters downstream from the rotor. In parallel to PIV, LDA measurements provided data for various rotor regimes, revealing the existence of three regular frequencies governing the development of different processes and instabilities in the rotor wake. The near wake is governed by stable organized vortical structures, comprising the base oscillation of the flow, which closely coincides with the blade frequency. Next, the transitional regime in the wake is generally characterized by the rotor rotation frequency, with a development of disturbances from the tip and root vorticies leading to vortex paring and further complex behaviour towards the fully breakdown of the initial vortex structure of the wake. In the far wake a constant frequency corresponding to the Strouhal number is found for the long-scale instabilities.

The results consistently indicate that the wake a few diameters downstream of the rotor has systematic precessing of the wake core and that the frequency of this precessing is about fd/U = 0.23 and is independent of the rotor speed. This Strouhal number is in good agreement with the well-known constant Strouhal number that usually characterizes the oscillation in wakes behind bluff bodies. From associated visualizations and reconstructions of the flow field, it was found that the dynamics of the far wake and the Strouhal number is associated with the precession (rotation) of a helical vortex core. The data indicate that the Strouhal number is independent of the rotor angular speed.

The main result achieved within this study is that the wake behind a wind turbine rotor always contains a wake which oscillates at a constant Strouhal number, associated with the precession of a helical vortex. Certainly an effect of inflow turbulence conditions on the frequency and amplitude of the far wake precession is of interest and should be investigated further. For a wind turbine operating under atmospheric wind conditions, the wake is subject to both wake meandering and precession. Hence, both phenomena should be taken into account when modeling the wake dynamics of wind turbines.

5. Acknowledgments

The present work has been carried out with the support of the Danish Council for Strategic Research for the project COMWIND (grant 2104-09-067216/DSF) and the Russian Science Foundation. The authors also express their thanks to K.E. Meyer for useful discussions and help in calibration of PIV equipments during experiments.

References

[1] Sørensen J N 2011 Instability of helical tip vortices in rotor wakes *J.Fluid Mech.* **682** 1–4
[2] Naumov I V, Rahmanov V V, Okulov V L, Velte C M, Meyer K E, Mikkelsen R F 2012 Flow diagnostics downstream of a tribladed rotor model *Thermophysics and Aeromechanics* **19(2)** 253-263
[3] Okulov V L, Naumov I N, Kabardin I, Mikkelsen R F, Sørensen J N 2012 Experimental investigation of the wake behind a model of wind turbine in a water flume (oral presentation) *Abs. TWIND*-2012 (Oldenburg, Germany, 9-11 October 2012)
[4] Sherry M, Sheridan J, Lo Jacono D 2013 Characterisation of a horizontal axis wind turbine's tip and root vortices *Experiments in Fluids* **54** 1417
[5] Ivanell S, Mikkelsen R, Sørensen J N, Henningson D 2010 Stability analysis of the tip vortices of a wind turbine *Wind Energy* **13** 705–715
[6] Felli M, Camussi R, Di Felice F 2011 Mechanisms of evolution of the propeller wake in the transition and far fields *J. Fluid Mech.* **682** 5-53
[7] Chamorro L P, Hill C, Morton S, Ellis C, Arndt R E, Sotiropoulos F 2013 On the interaction between a turbulent open channel flow and an axial-flow turbine *J. Fluid Mech.* **716** 658-670
[8] Iungo G V, Viola F, Camarri S, Porté-Agel F, Gallaire F 2013 Linear stability analysis of wind turbine wakes performed on wind tunnel measurements *J. Fluid Mech.* **737** 499-526
[9] Medici D, Alfredsson P H 2008 Measurements behind model Wind Turbine: further evidence of wake meandaring *Wind Energy* **11** 211–217
[10] Zhang W, Markfort C D, Porte´-Agel F 2012 Near-wake flow structure downwind of a wind turbine in a turbulent boundary layer *Exp. Fluids* **52** 1219–1235
[11] Achenbach E 1974 Vortex shedding from spheres *J. Fluid Mech.* **62(2)** 209-221
[12] Nakamura Y 1996 Vortex shedding from bluff bodies and a universal Strouhal number *Journal of Fluids and Structures* **10(2)** 159–171
[13] Meyer K E, Naumov I V, Kabardin I, Mikkelsen R, Sørensen J N 2013 PIV in a model wind turbine rotor wake Proc. The 10th International Symposium on Particle Image Velocimetry (Delft, Netherlands, 1-3 July 2013) A114
[14] Glauert H 1935 Airplane propellers *Aerodynamic Theory* ed. W.F.Durand (Berlin: Springer) **IV**
[15] Larsen G C, Aagaard Madsen H, Bingöl F, Mann J, Ott S, Sørensen J N, Okulov V, Troldborg N, Nielsen M, Thomsen K, Larsen T J, Mikkelsen R 2007 Dynamic wake meandering modeling *Risø Report* 1607(EN) (Publisher Risø National Laboratory, ISBN: 978-87-550-3602-4) 84
[16] Okulov V L, Naumov I V, Sørensen J N 2007 Optical diagnostics of intermittent flows *Technical Physics* **77** 47-57
[17] Naumov I V, Okulov V L, Meledin V G 2013 Method and devise of no contact optical-laser diagnostics of unsteady vortex flows *Patent RU 2498319*